

Once-for-All: 3D Auxiliary Graph Driven by Heterogeneous GAT for Multi-Tenant Adaptive Slicing in Multi-Layer Computing Power Networks

Huangxu Ma⁽¹⁾, Jiawei Zhang^{(1)*}, Zhiquan Gu⁽¹⁾, Daniel C. Kilper⁽²⁾, Yuefeng Ji^{(1)*}

⁽¹⁾ State Key Lab of Information Photonics and Optical Communications, Beijing University of Posts and Telecommunications (BUPT), Beijing, China, *zjw@bupt.edu.cn, jyf@bupt.edu.cn.

⁽²⁾ CONNECT Centre, Trinity College Dublin (TCD), Dublin, Ireland.

Abstract *Once-for-All, a heterogeneous graph attention network (HGAT)-driven three-dimensional auxiliary graph (3DAG) method for multi-tenant adaptive slicing, is studied in multi-layer computing power network testbed experiments. The holistic modelling by 3DAG and heterogeneous perception of HGAT enable 14% energy savings that generalize across requests and networks. ©2023 The Author(s)*

Introduction

Widespread application of AI has promoted the rapid development of cloud & edge computing. Recently, the computing power network (CPN) concept was introduced as a potential evolution of mobile edge computing to enable more efficient scheduling of distributed computing resources in networks^[1,2]. With the ongoing miniaturization of pluggable, high-speed optical modules^[3], and the disaggregation of software and hardware for reconfigurable optical add/drop multiplexers (ROADMs)^[4], IPoWDM is regaining popularity^[5] for interconnecting computing resources. A crucial technique for such multi-layer CPN is the use of network slicing. Multiple virtual operators rent physically/ logically isolated servers and wavelengths from the network infrastructure provider through slicing. In practice, pre-determining the slice structure is a challenge due to the uncertainty of service function chain (SFC) requests from tenants. An efficient way is to isolate slicing resources during SFC deployment, and implement an adaptive multi-tenant slicing scheme. Each SFC may either reuse the shared resources of its tenant or reserve new resources. A great challenge for the infrastructure provider lies in how to allocate slices for tenants and deploy diverse SFCs in slices to ensure energy-efficient networking, especially in the multi-layer CPN case.

Against the above problem, a series of “alternate” deployment methods (ALTs) have been proposed, including heuristic^[6] and deep reinforcement learning (DRL)^[7-9]. The majority of ALTs split the SFC deployment into two subproblems and run alternately: virtual node (VN) embedding and virtual link (VL) routing. In general, the VN embedding is solved by node ranking^[10] based on the remaining resources^[6] or neural networks^[7], while VL routing along with lightpath establishment is implemented through the auxiliary graph (AG)^[11]. ALTs are effective in

simplifying this complicated problem. However, the two separate subproblems can only achieve their local optimization, while the strong correlation between them limits the global optimization due to the lack of a holistic view.

This paper describes an adaptive multi-tenant slicing engine in a multi-layer CPN scenario, which deploys all VNs & VLs of each SFC with a single decision (Once-for-All, OFA). A three-dimensional AG (3DAG) is proposed to model the whole process of SFC deployment, while a DRL agent is responsible for optimizing its edge weights. In particular, a novel neural network based on heterogeneous graph attention network (HGAT)^[12] is incorporated into the DRL agent to surpass the state-of-the-art GAT^[13] by perceiving potential and rented resources differently. We demonstrate and compare OFA with baselines including ALTs and 3DAG with manually defined weights in a testbed. Results indicate that OFA enabled by HGAT (OFA-HGAT) leads to >14% CPN energy savings. In addition, OFA is shown to generalize well across requests and networks.

Problem Modelling Based on 3DAG

SFC deployment in a multi-layer CPN is a complicated optimization issue, which requires joint decisions across IP, wavelengths, and

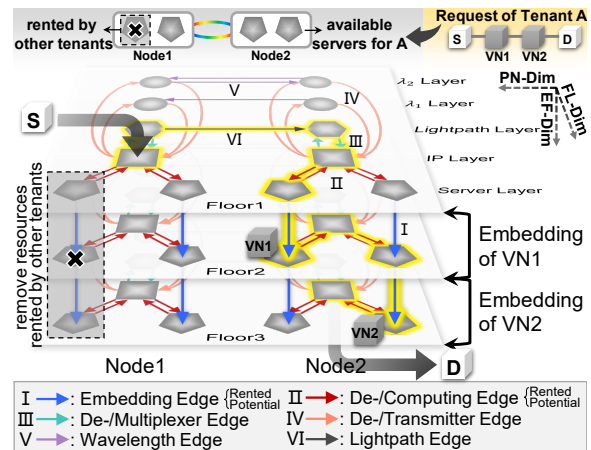


Fig. 1: Three-Dimensional Auxiliary Graph.

servers. An example of 3DAG for modelling such issues (Fig. 1) is the deployment of an SFC with $N = 2$ VNs in a 2-node multi-layer CPN with 2-servers/node and 2-wavelengths/link. The three dimensions in the 3DAG are the physical node dimension (PN-Dim), the functional layer dimension (FL-Dim), and the embedding floor dimension (EF-Dim). The newly introduced server layer, together with the IP layer, lightpath layer, and wavelength layer, forms the entire FL-Dim. The vertices in 3DAG are linked by eight kinds of edges, including rented/potential embedding edges (EBE(Rent./Pot.)), rented/potential de-/computing edges (De-/CPE(Rent./Pot.)), de-/multiplexer edges (De-/MXE), de-/transmitter edges (De-/TRE), wavelength edges (WLE), and lightpath edges (LPE). When initializing for one SFC, resources rented by others are removed, the embedding floor is then replicated into $N+1$ copies in EF-Dim.

By applying 3DAG, the SFC deployment is simplified as a dynamic multistage graph shortest path problem between the source vertex of the IP layer in Floor 1 and the destination vertex in Floor ($N+1$), which can be addressed by dynamic programming and Dijkstra. Specifically, the shortest path from the source vertex to each server vertex on each floor is calculated floor-by-floor, and the newly activated lightpaths and servers are updated to the next floor until the destination. A time-varying scenario is considered and each SFC is assumed to hold a dynamic demand for 24 hours. For each floor, those remaining resources that do not meet the demand during all 24 hours are removed. Different optimization goals can be achieved by modifying the edge weights of 3DAG.

OFA Algorithm

In OFA, a DRL with an HGAT-enabled agent is introduced to dynamically modify the edge weights of 3DAG for each request, as shown in Fig. 2. The optimized 3DAG is then responsible for the complete deployment of the SFC.

• Interface Design:

(1) **State**: the CPN state includes the remaining computing and bandwidth resources, except those rented by other tenants. The time-varying requirements of each VN and VL, and the

one-hot encoded source node, destination node, and tenant number compose the SFC state. (2) **Action**: the action specifies eight types of edge weights selected from a continuous action space. (3) **Reward**: to achieve energy-efficient networking, an energy consumption model^[14-16] for multi-layer CPN is established in Fig. 2(b). When an SFC is deployed by the optimized 3DAG, reward r in Eq. (1) is fed back, which is a negative value of the added energy consumption. θ, μ, γ are the number of newly activated servers, lightpaths, and wavelengths.

$$r = -(99.75\theta + 27.5\mu + \gamma) \quad (1)$$

• HGAT-Enabled Agent

Considering the different contributions of the rented and potential servers/lightpaths to the energy consumption, we transform CPN into a hetero-graph, in which rented and potential resources are assigned different attributes. HGAT is then used for efficient feature extraction of the CPN state. HGAT is characterized by the synergy of node-level and relation-level attention. Node-level attention aims to learn the importance of neighbouring nodes, while relation-level attention learns the relationship among resources with different attributes.

As shown in Fig. 2 (a), the workflow of the HGAT-enabled agent consists of four parts. (1) **Relation dividing**: after removing resources rented by others, CPN represented as a hetero-graph is divided into three subgraphs according to the attributes, including a potential subgraph with potential resources, a rented subgraph with rented resources, and a hybrid subgraph with all. For each subgraph, those computing/bandwidth features not belonging to it are filled with -1. (2) **Node-level attention**: for each subgraph G^r , the node-level attention weight α_{ij}^r from node i to j is calculated by Eq. (2), which takes into account both their node features H_i^r, H_j^r and the edge feature M_{ij}^r . The updated message $H_i^{r'}$ is given in Eq. (3) by the weighted sum of all neighbours \mathcal{N}_i . (3) **Relation-level attention**: attention weight $\beta_i^{r,q}$ between each two subgraphs G^r, G^q of node i is obtained by Eq. (4). Node messages considering relationships between subgraphs are updated by Eq. (5). The corresponding node messages of all subgraphs are finally

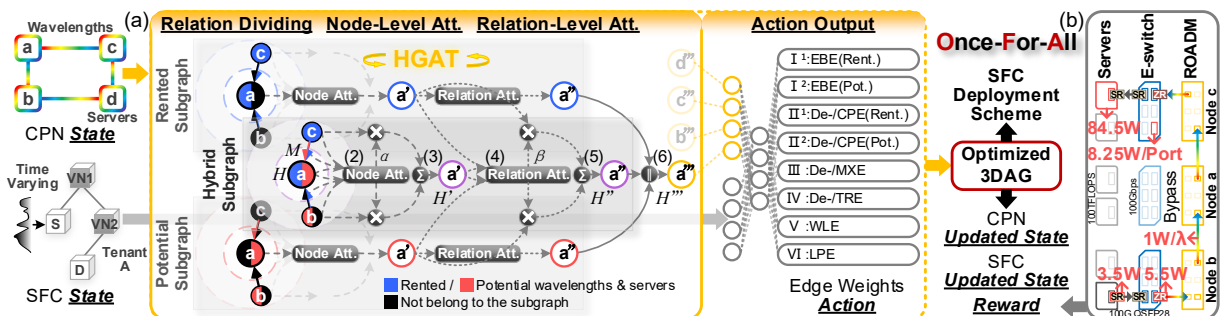


Fig. 2: The overall structure of OFA (a) HGAT-enabled agent; (b) Energy consumption model for multi-layer CPN.

concatenated by Eq. (6). \vec{a}, \vec{b}, W are trainable matrixes. (4) **Action output**: after rounds of message updates by HGAT, node messages in CPN and the SFC state are concatenated and fed into hidden layers. The output values are scaled to $[0, 250]$ as the optimized 3DAG edge weights.

$$\alpha_{ij}^r = \text{Softmax}_j^r(\text{LeakyReLU}(\vec{a}^{rT} W_1^r [H_i^r || M_{ij}^r || H_j^r])) \quad (2)$$

$$H_i^{r'} = \sum_{j \in \mathcal{N}_i} \alpha_{ij}^r W_2^r H_j^r \quad (3)$$

$$\beta_i^{r,q} = \text{Softmax}_q^i(\text{ReLU}(\vec{b}^{iT} W_3^i [H_i^{r'} || H_i^{q'}])) \quad (4)$$

$$H_i^{r''} = \sum_{q \in \mathcal{R}} \beta_i^{r,q} W_4^q H_i^{q'} \quad (5)$$

$$H_i^{r'''} = ||_r^R H_i^{r''} \quad (6)$$

We train the agent with the soft actor-critic algorithm (SAC)^[17]. The HGAT adopts 4 layers for node-level attention with 3 heads and 64 hidden features. Relation-level attention uses 4 heads and 16 output features. 4 hidden layers with (512, 256, 128, 8) neurons are attached.

Experimental Setup and Results Analysis

We verify the performance in our multi-layer network testbed^[7,18] as shown in Fig. 3 (a)(d), which contains 9 hybrid optical-electrical switching nodes. 4×10 Gbps wavelengths interconnect the ROADMs. A network test platform connected to the electronic switch (E-switch) generates VL traffic. Each node deploys two simulated 10 TFLOPS servers. SFC requests from three physically isolated tenants share the CPN infrastructure. The number of virtual nodes is random in $[1, 5]$, and the time-varying SFC requirements are scaled to $[0, 1.5]$ Gbps/TFLOPS.

We compare OFA-HGAT with five baselines, including OFA enabled by GAT (OFA-GAT), ALT-HGAT, ALT-GAT, 3DAG with fixed edge weights set as [EBE(Pot.): 99.75, TRE: 27.5/2, WLE: 1, others: 0], and node ranking with AG. Fig. 3 (c) shows OFA-HGAT achieves the best convergence. 3DAG optimizes the multi-tenant SFC deployment from a holistic view. Meanwhile, HGAT heterogeneously perceives resources with different attributes and achieves superior

performance in both ALT and OFA. The convergent algorithms are used for the deployment of 50 SFCs accompanied by adaptive slicing for multi-tenants. As illustrated in Fig. 3(c), OFA-HGAT reduces energy consumption by 14% compared to ALT-GAT, with the two key components of 3DAG and HGAT contributing benefits of 9% and 5%, respectively. For the fixed 3DAG, 21% energy reduction is achieved by OFA-HGAT, which can obtain the optimal edge weights for each SFC by perceiving the dynamic states of the CPN and SFC. Frequent optical-electrical-optical (OEO) conversions in multi-layer networks lead to additional delay and energy consumption. Fig. 3(f) shows that OFA-HGAT also achieves fewer OEO conversions. Generalization across requests and networks was also verified. We randomly generate 20 datasets with 50 SFCs each. The results in Fig. 3(g) show that OFA-HGAT retains energy savings when generalizing to other datasets. We save the HGAT weights that converged in the 9-node CPN and load them into a 14-node CPN with 2-servers/node, 5-wavelengths/link, and 100 SFCs from 5 tenants as shown in Fig. 3(e). The results in Fig. 3(h) demonstrate that preserving the HGAT weights leads to faster convergence with similar energy savings compared to retraining the HGAT model.

Conclusions

We studied OFA for SFC deployment with adaptive slicing in multi-tenant, multi-layer CPNs. Experimental results validated that OFA achieves superior performance through the effective combination of 3DAG and HGAT, including 14% energy savings, fewer OEO conversions, and generalization across requests and networks.

Acknowledgements: This work is supported by the NSFC project 62271078, the State Key Laboratory of IPOC (BUPT) (No. IPOC2022ZT11) P.R. China, the Fundamental Research Funds for the Central Universities (NO.2023RC15), the BUPT Excellent Ph.D. Students Foundation (CX 2022105), the BUPT Innovation and Entrepreneurship Support Programs (2022-YC-A022), Xiaomi Young Talents Program, and SFI under grant No. 13/RC/2077 P2.

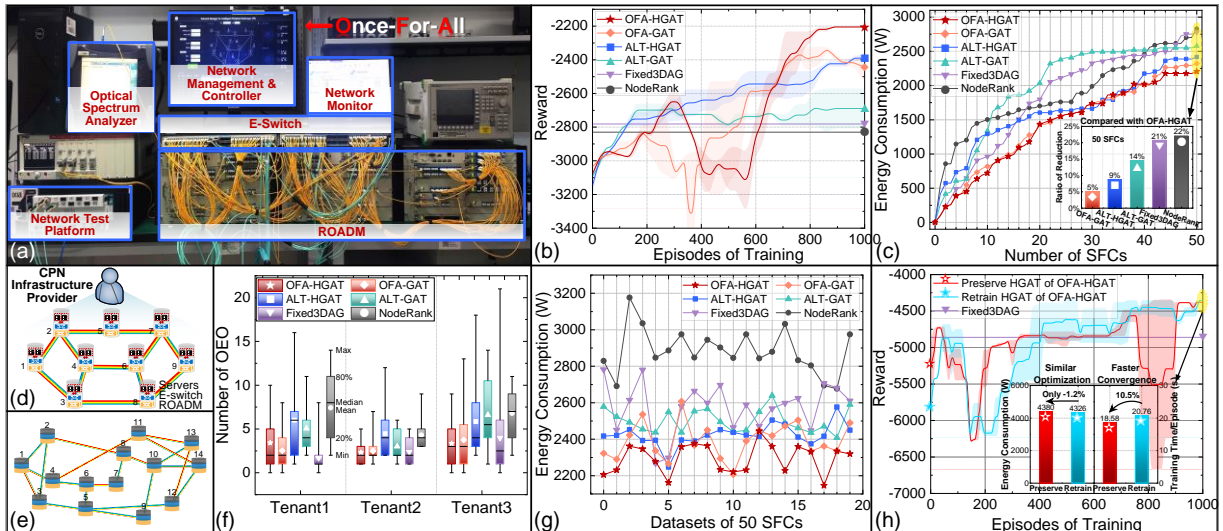


Fig. 3: (a) Multi-layer network testbed; (b) Convergence processes; (c) Energy consumption vs. No. of SFCs; (d) 9-node topology; (e) 14-node topology; (f) No. of OEO per SFC vs. tenant (g) Generalization across requests; (h) Generalization across networks.

References

- [1] ITU-T, "Y.2501 Computing Power Network – Framework and Architecture", 2021, Available: <https://www.itu.int/rec/T-REC-Y.2501-202109-I>.
- [2] B. Lei and G. Zhou, "Exploration and practice of Computing Power Network (CPN) to realize convergence of computing and network," in *Optical Fiber Communications Conference and Exhibition*, 2022: Optica Publishing Group, pp. 1-3, DOI: <https://doi.org/10.1364/OFC.2022.M4A.2>.
- [3] T. Tanaka, "Adaptive Traffic Grooming Using Reinforcement Learning in Multilayer Elastic Optical Networks," in *Optical Fiber Communications Conference and Exhibition*, 2023: Optica Publishing Group, pp. 1-3, Available: <https://opg.optica.org/abstract.cfm?uri=OFC-2023-Tu2D.6>.
- [4] M. Birk, O. Renais, G. Lambert, C. Betoule, G. Thouenon, A. Triki, D. Bhardwaj, S. Vachhani, N. Padi, and S. Tse, "The openroadm initiative," *Journal of Optical Communications and Networking*, vol. 12, no. 6, pp. C58-C67, 2020, DOI: <https://doi.org/10.1364/jocn.380723>.
- [5] A. M. L. de Lerma, J.-F. Bouquier, J. A. Gómez, S. Melin, R. Diaz, O. G. de Dios, J. P. Fernández-Palacios, K. Coskun, R. Bozaci, and S. Hill, "Unified SDN Control and Management of Disaggregated Multivendor IP over Open Optical Networks," in *European Conference on Optical Communication*, 2022: IEEE, pp. 1-4, Available: <https://opg.optica.org/abstract.cfm?uri=ECEOC-2022-We2B.1>.
- [6] J. Zhang, Y. Ji, M. Song, H. Li, R. Gu, Y. Zhao, and J. Zhang, "Dynamic virtual network embedding over multilayer optical networks," *Journal of Optical Communications and Networking*, vol. 7, no. 9, pp. 918-927, 2015, DOI: <https://doi.org/10.1364/jocn.7.000918>.
- [7] H. Ma, J. Zhang, Z. Gu, H. Yu, T. Taleb, and Y. Ji, "DeepDefrag: Spatio-Temporal Defragmentation of Time-Varying Virtual Networks in Computing Power Network based on Model-Assisted Reinforcement Learning," in *European Conference on Optical Communication*, 2022: IEEE, pp. 1-4, Available: <https://opg.optica.org/abstract.cfm?uri=ECEOC-2022-Tu5.59>.
- [8] Z. Yan, J. Ge, Y. Wu, L. Li, and T. Li, "Automatic virtual network embedding: A deep reinforcement learning approach with graph convolutional networks," *IEEE Journal on Selected Areas in Communications*, vol. 38, no. 6, pp. 1040-1057, 2020, DOI: <https://doi.org/10.1109/jsac.2020.2986662>.
- [9] M. Lu, Y. Gu, and D. Xie, "A dynamic and collaborative multi-layer virtual network embedding algorithm in SDN based on reinforcement learning," *IEEE Transactions on Network and Service Management*, vol. 17, no. 4, pp. 2305-2317, 2020, DOI: <https://doi.org/10.1109/tnsm.2020.3012588>.
- [10] X. Cheng, S. Su, Z. Zhang, H. Wang, F. Yang, Y. Luo, and J. Wang, "Virtual network embedding through topology-aware node ranking," *ACM SIGCOMM Computer Communication Review*, vol. 41, no. 2, pp. 38-47, 2011, DOI: <https://doi.org/10.1145/1971162.1971168>.
- [11] H. Zhu, H. Zang, K. Zhu, and B. Mukherjee, "A novel generic graph model for traffic grooming in heterogeneous WDM mesh networks," *IEEE/ACM Transactions On Networking*, vol. 11, no. 2, pp. 285-299, 2003, DOI: <https://doi.org/10.1109/tnet.2003.810310>.
- [12] T. Yang, L. Hu, C. Shi, H. Ji, X. Li, and L. Nie, "HGAT: Heterogeneous Graph Attention Networks for Semi-Supervised Short Text Classification," *ACM Transactions on Information Systems*, vol. 39, no. 3, pp. 1-29, 2021, DOI: <https://doi.org/10.1145/3450352>.
- [13] P. Veličković, G. Cucurull, A. Casanova, A. Romero, P. Lio, and Y. Bengio, "Graph attention networks," in *International Conference on Learning Representations*, 2018, pp. 1-12, DOI: <https://doi.org/10.48550/arXiv.1710.10903>.
- [14] Cisco. "Cisco Nexus 9500 Series Switches Data Sheet" [Online] Available: <https://www.cisco.com/c/en/us/products/collateral/switches/nexus-9000-series-switches/datasheet-c78-729404.html>.
- [15] Cisco. "Cisco 100GBASE QSFP-100G Modules Data Sheet" [Online] Available: <https://www.cisco.com/c/en/us/products/collateral/interfaces-modules/transceiver-modules/datasheet-c78-736282.html>.
- [16] SPEC. "All Published SPECpower_ssj2008 Results" [Online] Available: https://www.spec.org/power_ssj2008/results/power_ssj2008.html.
- [17] T. Haarnoja, A. Zhou, P. Abbeel, and S. Levine, "Soft actor-critic: Off-policy maximum entropy deep reinforcement learning with a stochastic actor," in *International conference on machine learning*, 2018: PMLR, pp. 1861-1870, DOI: <https://doi.org/10.48550/arXiv.1801.01290>.
- [18] Z. Chen, J. Zhang, B. Zhang, R. Wang, H. Ma, and Y. Ji, "ADMIRE: demonstration of collaborative data-driven and model-driven intelligent routing engine for IP/optical cross-layer optimization in X-haul networks," in *Optical Fiber Communications Conference and Exhibition*, 2022: Optica Publishing Group, pp. 1-3, DOI: <https://doi.org/10.1364/ofc.2022.m3f.4>.